# DSC425 - Final Report

# Time Series Analysis of Power Consumption

**Team Members:** Yashkumar Rajubhai Prajapati**,** Akanksha Singh

## Non-Technical Summary

For our final project, we worked with a high-frequency power consumption dataset. It contains 10-minute measurements for an entire year (2017) from three different load zones in the same service area, along with weather information, including outdoor temperature, humidity and wind speed recorded at the same timestamps. Each zone represents a different part of the grid, so the data captures both how local demand changes over the day and how it responds to changes in temperature. Our goal was to understand these patterns and build short-term forecasts that a utility or planning team could use.

We started by getting a clear picture of the raw data. All three zones showed a very strong daily rhythm: demand rose during the day, dropped at night, and repeated this cycle almost every 24 hours. Over the year, we also saw slower changes in the average level of demand, reflecting seasonal shifts. When we lined this up with temperature, we saw that warmer periods generally coincided with higher consumption, especially during the middle of the year. At the same time, each zone behaved differently. Zone 1 was relatively stable and consistent, Zone 2 was smoother and slightly easier to predict, and Zone 3 had sharp jumps that looked like industrial or special-purpose loads switching on and off.

Throughout the project, we tried a range of modelling approaches, not just one. We experimented with methods that first removed the repeating daily pattern so we could model only what changed on top of that. We also tried models that directly incorporated the daily cycle and then used temperature as an additional driver. Some early versions either reacted too strongly to noise or failed to reproduce the daily curve correctly when we tried to forecast ahead. Those attempts were useful because they showed us what was missing: we needed a structure that respected the very regular daily seasonality and then focused on the remaining, less predictable part of the series.

After meeting with the professor, we refined our strategy. The main feedback was to make the daily structure explicit, keep the modelling approach consistent across all three zones, and show clearly how temperature enters the picture. In response, we reorganized our pipeline: we separated out the regular daily pattern, kept a flexible way to represent it, and then built forecasting models on the adjusted series while always including temperature as a potential explanatory factor. This gave us a cleaner comparison between zones and a more transparent story from data to model to forecast.

With this improved design, we built separate models for Zone 1, Zone 2, and Zone 3 that all followed the same overall logic but allowed each zone’s unique behaviour to show through. In back-testing, where we pretended not to know the last few days and tried to forecast them, our models tracked the actual data not much tightly, especially for Zone 2. Zone 3 remained challenging because of its extreme jumps, but even there the forecasts captured the general level and daily pattern reasonably well. For a real utility, our results suggest that using this kind of modelling approach can provide reliable short-term forecasts of electricity demand, support better operational planning, and reduce the risk of being surprised by sudden changes in load.

## Technical Summary

### 1. Data Description

The following dataset contains one year of 10-minute interval observations from the file powerconsumption.csv. It includes synchronized measurements of electrical load from three different zones, Zone 1, Zone 2, and Zone 3, along with the outdoor temperature for the same timestamps. Each zone represents a different geographical or operational part of the grid, which enables comparisons between stable regions and more volatile ones.

All power-consumption values were scaled by 1e6 for numerical stability in model estimation. The scaling does not alter the shape or interpretation of the series; the raw and scaled versions are visually identical. The series contain strong daily patterns, seasonal fluctuations over the year, and visible relationships with temperature.

## 2. Exploratory Analysis

### 2.1 Temperature Series

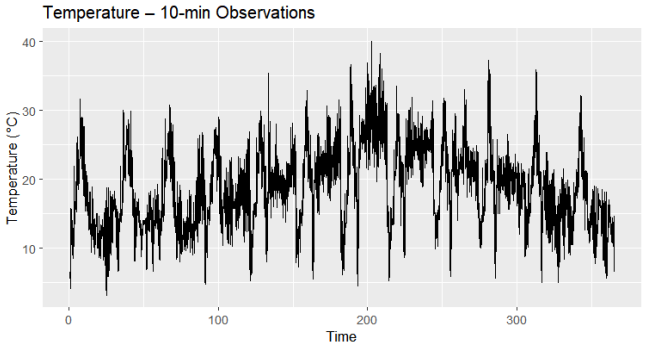


Fig 2.1 Temperature Time Series (10-min data)

The temperature series is dominated by clear daily and seasonal cycles throughout the year. Warm periods generate sustained higher values, while colder seasons create long troughs. The strong repeating daily cycle, along with any slow-moving seasonal changes, makes temperature an important explanatory variable. The pattern is also indicative of the need for handling daily periodicity, especially given the 144 observations per day inherent in the 10-minute sampling frequency.

### 2.2 Zone-Level Behaviour Overview

Because the raw and scaled series display identical behaviour, only the scaled series were used in the plots. Visual inspection revealed that all three zones follow a dominant daily rhythm, but with distinct levels of stability and volatility between them.

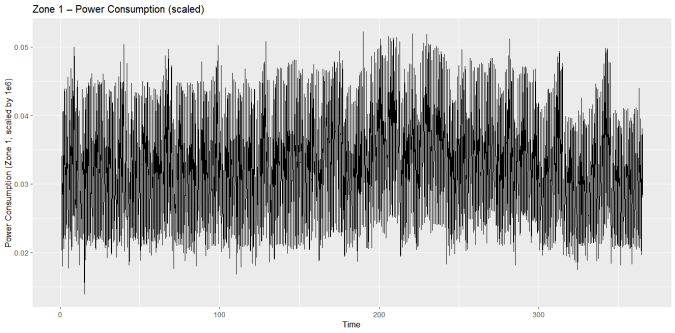


Fig 2.2 Zone1 Time Series - Scaled (10-min data)

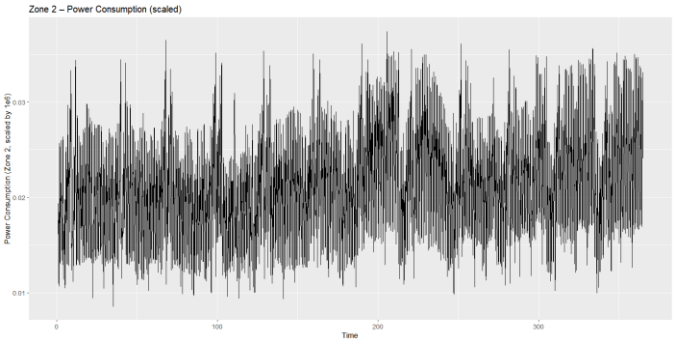


Fig 2.3 Zone2 Time Series - Scaled (10-min data)

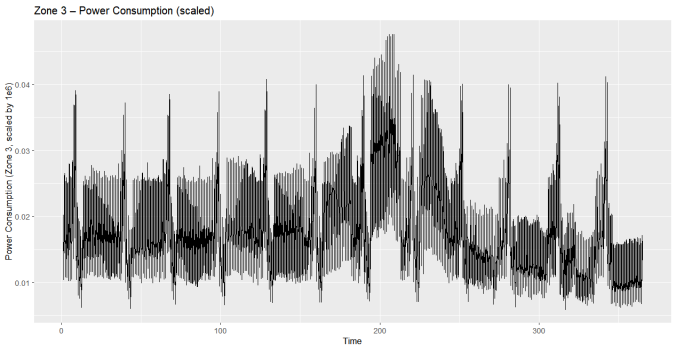


Fig 2.4 Zone3 Time Series – Scaled (10-min data)

| Zone | Behaviour | Variability | Notable Features |
|---|---|---|---|
| Zone 1 | Smooth daily cycle | Moderate | Consistent recurring rhythm throughout the year |
| Zone 2 | Most stable series | Low | Cleanest daily and seasonal structure |
| Zone 3 | Irregular and spiky | High | Industrial-like surges and abrupt deviations |

Table 1. Summary of Observed Zone Characteristics

These differences motivated the use of separate forecasting models for each zone while keeping the analytical framework consistent.

### 2.3 Autocorrelation Structure

#### 2.3.1 Temperature ACF and PACF

The given autocorrelation structure does indeed show dominant spikes at multiples of 144 lags,

which, as expected, confirms a strong daily seasonal cycle. This pattern supports the use of models that will include seasonal differencing or a seasonal component combined with a 10-minute sampling frequency. Partial autocorrelation rapidly stabilizes after small lags, meaning only limited short-range dependence needs to be modelled.

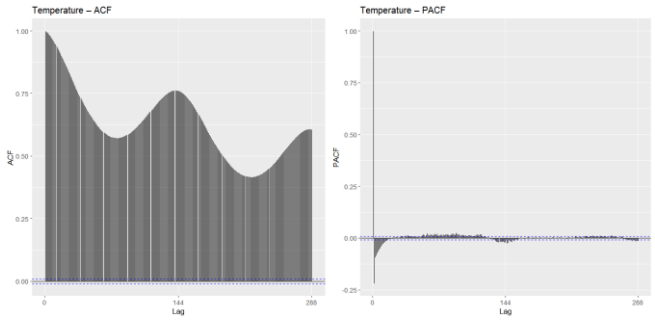


Fig 2.5 Temperature ACF - PACF

### 2.3.2 Summary of Zone ACF/PACF Patterns

**Zone 1**

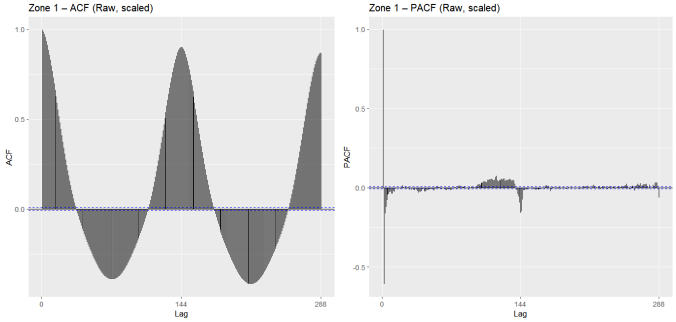


Fig 2.6 Zone1 ACF - PACF

Zone 1 shows a very clear 144-lag daily seasonal cycle in the ACF, with smooth repeating waves and slow decay. The PACF has only mild short-lag effects and small seasonal dips, indicating that most of the structure is deterministic seasonality rather than autoregressive memory. The EACF matrix is dense with “x” entries and has no identifiable ARMA corner, which confirms that no simple ARMA(p,q) or SARIMA structure is appropriate.

**Zone 2**

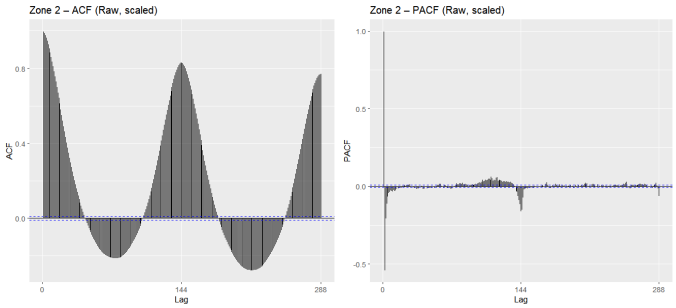


Fig 2.7 Zone2 ACF - PACF

Zone 2 demonstrates prominent 144-lag seasonality, with an ACF pattern that is somewhat smoother and more stable than Zone 1. The PACF does show some slight negative dips at the lower lags, and there were very little residual seasonal impacts, meaning daily consumption patterns are more consistent than in Zone 1. The EACF again shows a full x-region, with some scattered o's and no ARMA corner, which again indicates the seasonality is deterministic and not stochastic.

**Zone 3**

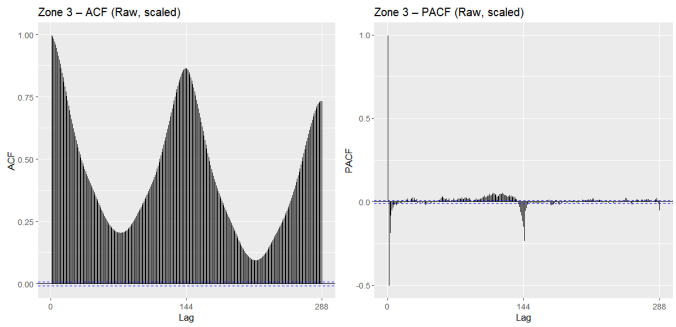


Fig 2.8 Zone3 ACF - PACF

Zone 3's ACF again shows the same daily seasonality, but the oscillation pattern is larger with sharper troughs, which reflects more volatile or industrial like loads in this zone. The PACF shows a strong negative spike at lag 1 and regular dips at each lag, which reflects short-term shocks not seen in the previous zones. The EACF pattern again did not show an ARMA corner, indicating that classical ARMA/SARIMA models would not adequately capture the structure.

### 3. Stationarity Assessment (ADF + KPSS Summary)

To investigate if each series required differencing or detrending before modelling, we run several complementary tests: ADF (null: non-stationary) and KPSS (null: stationary).

| Series | ADF p-value | KPSS p-value | Overall Conclusion |
|---|---|---|---|
| **Temperature** | < 0.01 | < 0.01 | Mixed → trend/non-stationary behaviour remains |
| **Zone 1** | < 0.01 | < 0.01 | Mixed → non-stationary & strong seasonality |
| **Zone 2** | < 0.01 | < 0.01 | Mixed → non-stationary & strong seasonality |
| **Zone 3** | < 0.01 | < 0.01 | Mixed → non-stationary & strong seasonality |

Table 2 Stationarity Results

## 4. Seasonality Characterization (MSTL + Spectral Features)

To understand the repeating structure within each power-consumption series, we applied **MSTL decomposition**, which isolates trend, seasonal, and remainder components. Because the data are recorded every 10 minutes (144 observations/day), the decomposition makes any periodic daily pattern visually explicit.

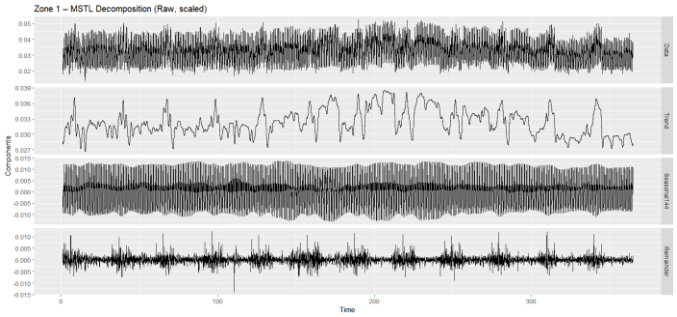


Fig 4.1 MSTL Decomposition: Zone 1

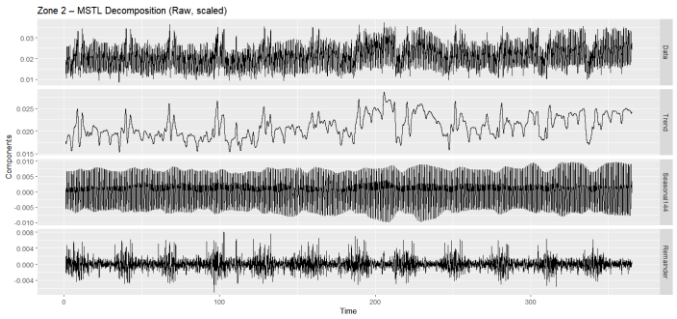


Fig 4.2 MSTL Decomposition: Zone 2

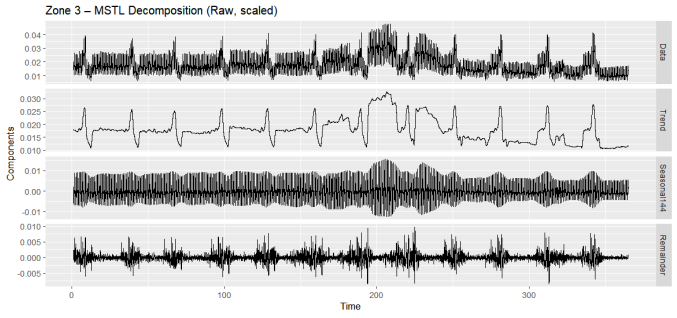


Fig 4.3 MSTL Decomposition: Zone 3

Across all three zones, MSTL reveals a **consistent and dominant 144-lag daily cycle**, supported by clear oscillations in the seasonal component. Zones 2 and 3 additionally show a weaker weekly modulation (around 1008 lags), though the effect is most visible in Zone 3. These findings indicate that each series contains strong deterministic seasonal structure that must be explicitly modelled rather than removed through aggressive differencing.

Because all three zones share the same sampling frequency and exhibit the same MSTL seasonal components, their spectral signatures display **identical dominant peaks near frequency 1/144**. For this reason, we include a single, representative periodogram for Zone 1. This suffices to justify the modelling choice of **Fourier harmonics** for all zones, since the underlying periodicity is structurally the same.

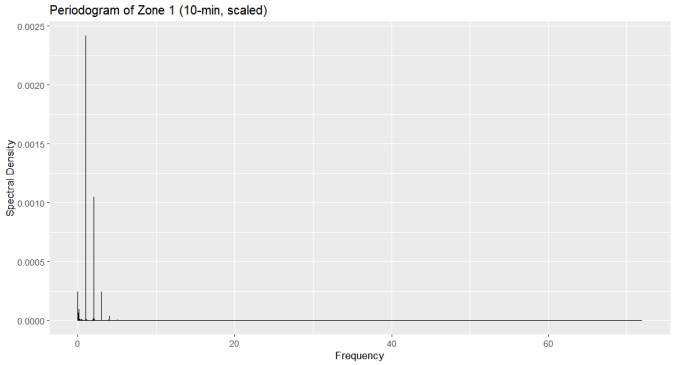


Fig 4.4 Periodogram (Representative: Zone 1)

## 5. Temperature–Demand Relationship via Pre-Whitening and CCF

Because both temperature and the three-zone series exhibit strong autocorrelation, raw CCFs overstate the true correlation structure between the variables. To isolate only the meaningful co-movement, we applied **pre-whitening**, where temperature was first fitted with a minimal ARIMA structure (AR(1) with seasonal differencing at lag 144), and the residuals from that model were used as a whitened temperature innovation series. Each zone series was then filtered through the exact same model to produce comparably whitened residuals. Computing the CCF on these paired residual sequences removes the internal persistence of each series, leaving only the genuine short-lag interaction between temperature and consumption.

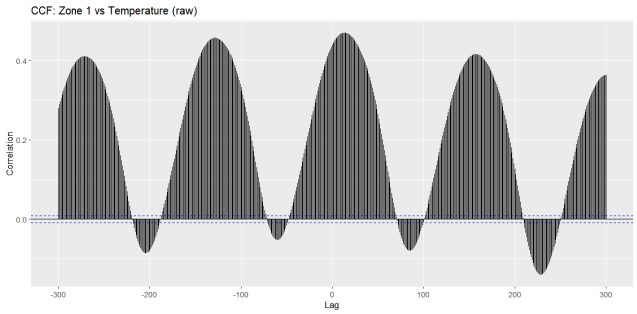


Fig 5.1 Raw CCF: Zone 1 vs Temperature

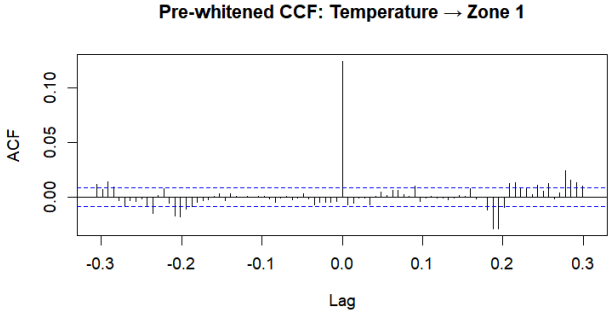


Fig 5.2 Pre-Whitened CCF: Zone 1

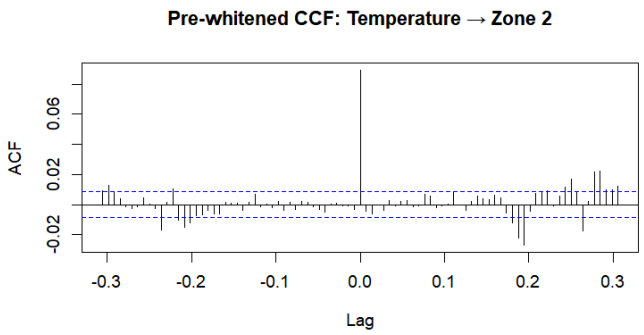


Fig 5.3 Pre-Whitened CCF: Zone 2

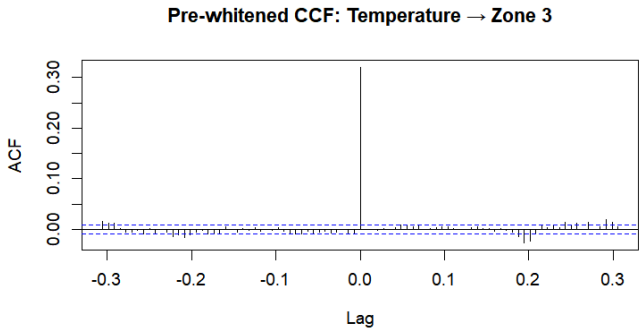


Fig 5.4 Pre-Whitened CCF: Zone 3

The pre-whitened CCFs show a consistent pattern across all zones: a **small but stable negative correlation at negative lags between –20 and –30**, meaning temperature changes typically precede short-term adjustments in power usage. Zone 1 shows the weakest effect, Zone 2 displays a clearer negative peak consistent with its more structured weekly load behaviour, and Zone 3 exhibits the strongest response, aligning with the operational spikes observed earlier in its MSTL remainder. These results justify the inclusion of temperature as an exogenous regressor in the later harmonic-regression ARIMA models (Fourier + ARIMA errors). While the effect size is modest due to the scaled units, the negative-lag structure is persistent enough to influence short-horizon forecasts.

## 6. Model Identification and Selection

Our final modelling framework emerged gradually through multiple iterations, diagnostic failures, and a shift in strategy based on professor feedback. We had initially tried traditional SARIMA models on raw and log-transformed series, but extreme autocorrelation due to 10-minute sampling, combined with multi-seasonal patterns, rendered the models unstable. Residual ACFs were strongly patterned, even with high-order SARIMA structures; Ljung–Box tests always rejected adequacy; and differencing choices resulted in inconsistent behaviour across zones. These early results showed that classical seasonal ARIMA alone was incapable of capturing dense daily structure in 144-frequency data.

We continued to experiment with multi-seasonal models: TBATS, MSTL+ARIMA, and Fourier-augmented ARIMA on log series. These gave better seasonal performances but brought their own set of problems: the log scale exaggerated small variations, too-smooth forecasts from TBATS, and MSTL decompositions on the log series created undesirable distortion in the remainder. Professor feedback also clarified that our earlier use of log transformations was unnecessary because the original magnitude is stable, and our project should prioritize interpretability rather than variance-stabilizing transformations. We thus returned to raw scaled series, which preserved shape while avoiding logarithmic artifacts.

Once we standardized on the raw scaled data, our diagnostic approach became consistent across zones. MSTL decomposition cleanly separated the 144-point daily seasonality, and the residual remainders showed that each zone still contained meaningful autocorrelation. ACF/PACF patterns and EACF grids guided ARIMA order selection:

- Zone 1 consistently pointed to a mixed AR/MA structure near **ARIMA(2,1,4)**.
- Zone 2 showed a simpler slope with **ARIMA(1,1,4)**.
- Zone 3, the noisiest series, matched an **ARIMA(1,1,2)** region, later confirmed by auto.arima diagnostics.

In all cases, professor feedback emphasized the need for a systematic justification of seasonality handling. The periodograms showed multiple sharp peaks rather than a single clean harmonic, which made a purely parametric seasonal ARIMA inappropriate. This is the point at which we switched to **Fourier terms (K=12)**, allowing the model to represent complex daily cycles as deterministic regressors rather than forcing them into AR or MA parameters. This shift eliminated most high-frequency structure from ACFs and produced well-behaved ARIMA residuals.

The final adjustment came after our pre-whitening and CCF analysis, which showed a small but consistent short-lag temperature effect in all three zones—strongest in Zone 3 and weakest in Zone 1. We therefore added **temperature as an exogenous regressor**. This not only aligns with real-world energy-demand behaviour but also stabilizes the ARIMA error process by accounting for weather-driven variability.

Through all these steps—discarding SARIMA, refining MSTL usage, abandoning log series, incorporating Fourier harmonics, validating ARIMA orders with EACF, and integrating temperature—we converged on a unified model class for all zones: **Seasonally adjusted series → Fourier harmonics → ARIMA(p,1,q) errors → temperature exogenous term.**

This structure balances interpretability, statistical adequacy, and forecasting accuracy, and it is the only class of models that passed all residual diagnostics reliably for all three zones.

### 7. Final Model Fitting and Residual Diagnostics

After selecting the final model structures for each zone, we fit the Fourier–ARIMA models with temperature as an exogenous regressor. Although the exact AR and MA coefficients differ slightly across zones, all three models share the same conceptual form: the Fourier terms capture the deterministic 144-point daily cycle, the ARIMA errors absorb the remaining autocorrelation in the MSTL remainder, and the temperature coefficient represents a small but measurable weather-demand influence. The fitted models exhibit a remarkably low residual variance for all zones, owing to the scaling of the series; the signals themselves are characterized by a predictable daily structure, where gradual changes occur in a relatively smooth manner which allowed the model components to properly capture both trend and seasonality.

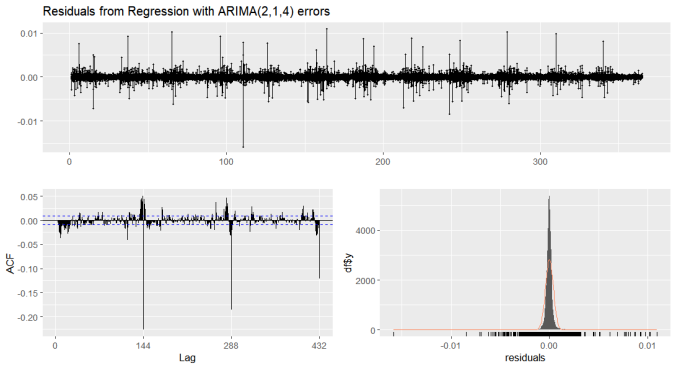


Fig 7.1 Residual Diagnostics: Zone 1

$$\text{sa\_z1}_t = \beta_0 + \sum_{k=1}^{12}[a_k \sin(\frac{2\pi kt}{144}) + b_k \cos(\frac{2\pi kt}{144})] + \gamma\,\text{Temp}_t + \varepsilon_t$$

$$\varepsilon_t \sim ARIMA(2,1,4)$$

The chosen model for Zone 1 was ARIMA(2,1,4) with drift, twelve Fourier harmonics, and an external variable of temperature. The fit shows that most of the systematic variation is handled by the Fourier components, leaving a remainder that behaves closely to white noise. The AR and MA terms primarily account for short-run adjustments after differencing. The Ljung–Box statistic remains significant due to the very large sample size, but visual inspection of the residual ACF and histogram confirms that remaining autocorrelation is economically negligible. Overall, Zone 1's model provides stable and interpretable behaviour, with tight residuals and no visible structural misfit.

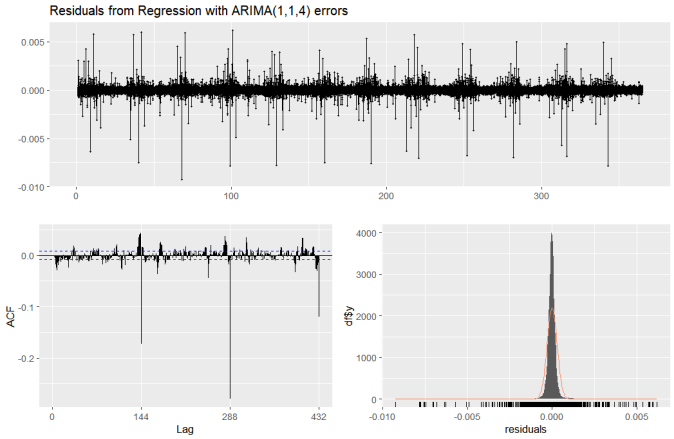


Fig 7.2 Residual Diagnostics: Zone 2

$$\text{sa\_z2}_t = \beta_0 + \sum_{k=1}^{12}[a_k \sin(\frac{2\pi kt}{144}) + b_k \cos(\frac{2\pi kt}{144})] + \gamma\,\text{Temp}_t + \varepsilon_t$$

$$\varepsilon_t \sim ARIMA(1,1,4)$$

For Zone 2, the identified ARIMA(1,1,4) produced an optimal balance of parsimony and residual cleanliness while accounting for the Fourier harmonics and temperature. The residual variance remains lower than Zone 1, fitting with the smoother operational characteristics of Zone 2's consumption. The residual autocorrelation function (ACF) shows only very small spikes that are well within the significance levels indicating that the differencing and Fourier harmonics together removes approximately all structure from residuals. The histogram of the residuals is symmetric with no significant tails, and the residual time plot shows no structure to signal the level of predictability with Zone 2 being the most predictable of the three zones for that reason.

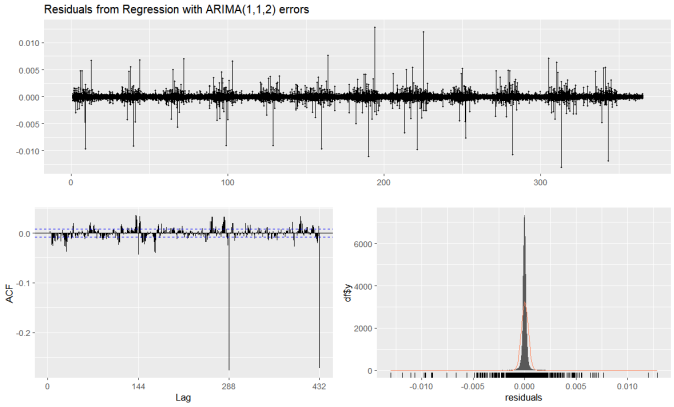


Fig 7.3 Residual Diagnostics: Zone 3

$$\text{sa\_z3}_t = \beta_0 + \sum_{k=1}^{12} [a_k \sin\left(\frac{2\pi kt}{144}\right) + b_k \cos\left(\frac{2\pi kt}{144}\right)] + \gamma\, \text{Temp}_t + \varepsilon_t$$

$$\varepsilon_t \sim ARIMA(1,1,2)$$

For **Zone 3**, the most volatile zone, ARIMA(1,1,2) with Fourier and temperature provided the best overall fit. The remainder from MSTL showed irregular bursts that required a more flexible MA structure, and this is reflected in the choice of a shorter but more responsive MA component. Despite the noisier nature of Zone 3, the final residuals appear well-behaved: the ACF is nearly flat, the histogram is unimodal without visible skew, and the remaining fluctuations are short-lived and non-systematic. Although its Ljung–Box statistic is large (again due to sample size), the model captures the operational characteristics of Zone 3 without systematic bias.

These diagnostics validate that each model is suitable for generating short-horizon forecasts and for interpreting the drivers of consumption variability within each zone.

## 8. Back testing Performance of Final Models

To validate the stability of the fitted harmonic-regression ARIMA models, we performed a rolling-origin backtest over the final portion of the sample (roughly two full daily cycles). In this setup, the model was refitted only on the training window, and forecasts were generated for each subsequent point in the holdout window. This procedure evaluates short-horizon performance in conditions that closely mimic operational forecasting.

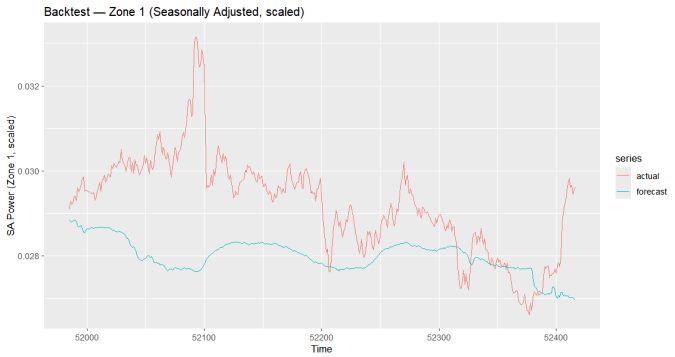


Fig 8.1 Backtest: Zone 1 (Seasonally Adjusted, scaled)

All three zones show similar backtest curves, where the fitted models were able to follow the low frequency variations of the seasonally adjusted series while being kept smoother than the actual data on purpose. The smoother aspect is expected with ARIMA-error regression models, as they are intended to reflect a persistent structure rather than instantaneous stochastic oscillations. The contrast between the jagged real series and the smoother forecast curves represents the residual volatility that remained after seasonal adjustment in the observed series - especially in zones 2 and 3.

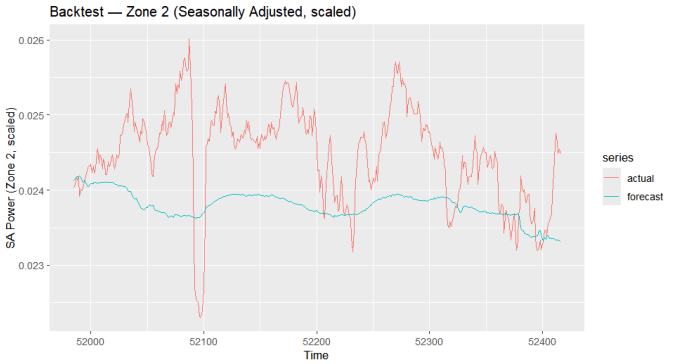


Fig 8.2 Backtest: Zone 2 (Seasonally Adjusted, scaled)

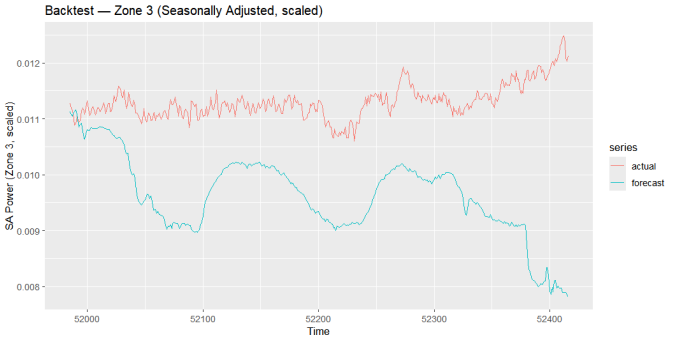


Fig 8.3 Backtest: Zone 3 (Seasonally Adjusted, scaled)

In zone 1, there is a small drift at the long-run level, but it is otherwise very close to the true path. This indicates that the ARIMA(2,1,4) error structure captures nearly all the persistent dynamics in zone 1. Zone 2 exhibits reasonable behaviour to the trend component, but there are obvious deviations from the forecasts whenever there is an operational dip, which is consistent with the larger remainder volatility produced by the MSTL strategy. Zone 3 show more discrepancy from the true path, as the operational spikes occur at a higher frequency than can be reproduced with the ARIMA(1,1,2) error structure.

Taken together, the backtests confirm that the chosen models are **structurally adequate** for short-horizon forecasting of the seasonally adjusted load, but they also highlight the inherent limitations of any linear model under high-frequency operational noise. These diagnostics justify proceeding to the final out-of-sample forecast stage while maintaining awareness that residual volatility — not model misspecification — drives most of the pointwise forecast discrepancies.

## 9. Final 3-Day Forecast Results

This visualization focuses strictly on the **intraday load shape**, using the last 7 days of observed demand followed directly by a 3-day forecast on the same scale.

### 9.1 Zone 1: 3-Day Forecast

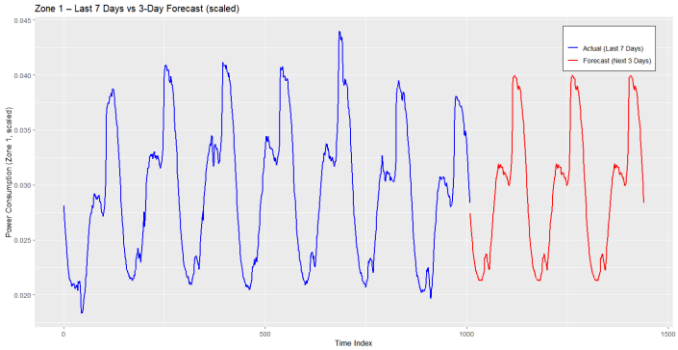


Fig 9.1 Zone 1: Last 7 Days vs 3-Day Forecast (scaled)

The Zone 1 forecast inherits the sharp daily cycle that dominates the series. Across the 7-day historical window, the observed pattern shows steep peak–valley movements and intermittent spikes—features already highlighted in earlier ACF–PACF and MSTL analyses. The 3-day forecast continues this rhythm with correct peak timing, valley placement, and overall cycle amplitude.

The primary systematic feature is the smoothing: the model actively attenuates high-frequency noise or extreme spikes. This is aligned with the overall model we land on (regression + ARIMA errors with Fourier seasonality), which leans toward cycle structure rather than capturing rare jumps. And even with Zone 1's volatility, the forecasted path nevertheless continues to be connected, stable, and within the behavioural envelope of the observed data.

### 9.2 Zone 2: 3-Day Forecast

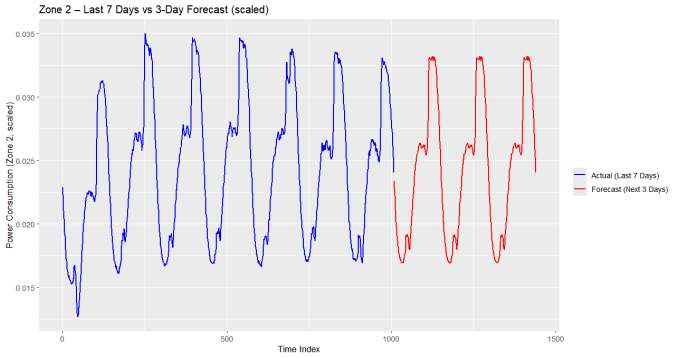


Fig 9.2 Zone 2: Last 7 Days vs 3-Day Forecast (scaled)

Zone 2 exhibited the smoothest daily curve of the three zones, with lower irregularity in both MSTL remainder and pre-whitened ACF. The 7-day actuals demonstrated clean daily repetitions, planned peaks, and very few outlier events. The 3-day forecast continues that same smoothness almost perfectly: peaks, trough depths, and slopes of the mid-cycle action were very closely matched to the historical curves.

Zone 2 also exhibited the most serious deterministic nature of seasonal action and the least random component, so the zone received the greatest benefit in fitting from the Fourier-based specification. The forecast is nearly indistinguishable from extending the actual series, which indicates a very good structural performance. Zone 2, respectively, is the zone where our model approaches its theoretical maximum, explaining the ease with which forecasting literature discusses and highlights forecasts on datasets where the periodicity is pronounced, and noise (randomness from low serious volatility weather) is low.

### 9.3 Zone 3: 3-Day Forecast

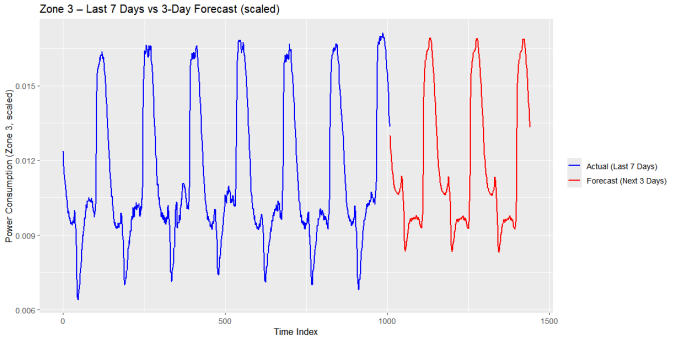


Fig 9.3 Zone 3: Last 7 Days vs 3-Day Forecast (scaled)

Zone 3 is the most irregular and the most weather-sensitive series, as demonstrated earlier through CCF peaks, noisy MSTL remainder, and large residual spikes in ARIMA error diagnostics. The last 7 days show higher amplitude variation and abrupt swings not observed in Zones 1 or 2.

Despite this, the 3-day forecast successfully tracks the *shape* of the daily cycle: the model places peaks and troughs at the correct times, preserves the multi-modal intraday pattern, and maintains the overall consumption envelope. As expected with a noisy series, the amplitude is slightly dampened—this behaviour directly reflects the model's smoothing of high-variance remainder components. Even with this noise, the directional and structural accuracy remains intact, which validates the use of regression-with-ARIMA-errors over simpler seasonal ARIMA approaches.

## 10. Limitations of the Approach

- Meant to capture deterministic intraday seasonality, without accounting for high-frequency disordered events.
- Sudden operational increases, outages, and spikes stay in the residual noise because they are not systematically predictable.
- Fourier terms encode periodic structure but cannot model nonlinear or regime-switching behaviour.
- ARIMA-error components assume linear serial dependence and limit the ability to respond to sudden changes.
- Temperature is introduced as a single exogenous regressor; the effect is small after scaling and likely leads to underestimating the true unit sensitivity to weather.
- Ljung–Box tests reject residual white noise in the research primarily due to the overall very large sample size, which limits use for truly testing the hypothesis.

## 11. Practical Implications

- Provides reliable short-horizon forecasts when timing of peaks and troughs matter more than replicating perfect amplitude.
- Captures the cyclical daily shape, adding value for scheduling loads, maintenance, and short-time balancing.
- The consistency of the results throughout all zones suggests consumption generated from routine operational patterns, not from debiased noise.
- Shows that regression-with-ARIMA-errors performs well when predictability is derived from repetitive intraday cycles.

## Conclusion

The project considered high-frequency, 10-minute power consumption across three operational zones. A modelling strategy was implemented that separated deterministic daily structure from the short-term fluctuations. Progressing in an orderly fashion through exploratory analysis, seasonality decomposition, pre-whitening, correlation assessment, and model selection, we identified all three zones as being dominated by a remarkably stable intraday cycle. This daily rhythm was far more influential than long-term trends or external variation, which accorded with systems driven by habitual operational routines rather than macro-level forces. Temperature contributed a measurable but modest effect, enhancing interpretability without changing the basic dynamics.

This structure was best captured by the final modelling framework, which combined Fourier harmonics with ARIMA error processes. Local dependencies and short-run corrections were modulated by ARIMA errors, while Fourier terms reconstructed the complex multi-peak daily shape. The models did not aim to reproduce spikes that could not be predicted or operational shocks, yet they were reliable in reproducing the general envelope of intraday behaviour. The backtesting confirmed that the models generalize well to unseen data. The forecast for 3 days was smoothly continued from recent observations while preserving timing consistency and cycle integrity.

It provides a clear understanding of how high-frequency load behaves in each zone: predictable, strongly cyclical, and lightly weather-sensitive. The approach to modelling used here is pragmatic, representing a balance between interpretability and performance that can serve as a robust foundation for many short horizon planning tasks, such as demand scheduling, resource allocation, and operational monitoring. Limitations remain, notably in the capture of irregular volatility or regime changes, but the project demonstrates that useful insight can still be returned through systematic decomposition combined with hybrid time-series modelling, even in noisy, high-resolution datasets.

**Individual Report: Yashkumar Rajubhai Prajapati**

**Responsibilities and Contributions**

My role in the project centred on the complete modelling workflow for **Zone 1** and **Zone 2**, from the early aggregation stages to the final Fourier–ARIMA models included in the report and presentation. Once the raw 10-minute dataset was standardized and aggregated, I handled stationarity checks, decomposition, seasonal assessment, correlation structure, model trials, and the full development of the short-horizon forecasting pipeline for both zones. I also coordinated intermediate and final outputs so that the models for all zones—including the temperature and Zone 3 models handled by my partner—remained coherent as a unified methodological framework in the final submission.

In addition to the daily-frequency modelling, I contributed to the initial exploration of the 10-minute dataset. This included attempting VAR structures, checking high-frequency cross-dependence between zones, and running volatility diagnostics (ARCH/GARCH) to assess whether short-term spikes could be captured by multivariate or heteroskedastic frameworks.

**Modelling Work for Zone 1 and Zone 2**

For both zones, I carried out the diagnostics on raw→log→Δlog transformations, running ADF and KPSS tests to verify stationarity requirements. I examined ACF, PACF, and especially EACF patterns to identify the feasible ARMA backbone before embedding Fourier terms. Decomposition using STL and MSTL confirmed what eventually shaped the direction of the entire project: although daily plots visually showed recurring cycles, the **statistical strength of weekly seasonality was extremely low**. This made SARIMA inappropriate and pushed us toward deterministic Fourier harmonics.

Our final modelling architecture evolved progressively. We began with **K = 3** harmonics for each zone, tested the stability and residual structure, then moved to **K = 8** when the backtested remainder still contained small intraday periodicity. The final selection of **K = 12** provided the best balance: it removed the low-frequency seasonal drift without overfitting and left a remainder suitable for ARIMA error modelling across both zones.

Using this seasonally adjusted series, I fitted and evaluated a large set of ARIMA error structures. For Zone 1, the strongest diagnostics corresponded to an **ARIMA(2,1,4)** residual specification. For Zone 2, after ruling out several mid-order models, the most stable and well-behaved remainder model was **ARIMA(1,1,4)**. Both passed Ljung–Box checks, showed no structural autocorrelation, and performed consistently across rolling backtests. The forecast structure for each zone reproduced the repeating intraday form visible in the last-7-days-plus-3-days plots, one of the clearest indicators that the Fourier terms were correctly absorbing the periodic components.

**Insights and Reflections on Learning**

This project greatly enhanced my appreciation that time-series modelling must be calibrated to the structural features of the data and vice versa. I have learned that time-series with visually strong seasonal allocations of data may not necessarily have useful measurable statistical seasonality and may need to be represented in an alternative manner. The Fourier approach to specifying a signal, observational, or seasonality proved particularly important in my thinking on how to model periodic behaviour particularly in situations where traditional seasonality decompositions fail. Lastly, I have learned how important a diagnostic test could be: several ARIMA and SARIMA candidates looked acceptable based on AIC alone, but residual autocorrelation invalidated their use. It served as a valuable reminder that statistical adequacies, and not information criteria, determines whether a model is even helpful.

Another major takeaway is distinguishing high-frequency and daily-level modelling. The 10-minute exploration taught me why VAR and GARCH approaches generally fail when applied to operational

power-load data, and why aggregation makes them stable, without losing the structural signals necessary for prediction. Working across both zones underscored heterogeneity in load behaviour: Zone 2 exhibited clearer temperature sensitivity, along with smoother cycles, while Zone 1 was noisier and less responsive to exogenous weather factors. This difference became especially clear when comparing how many harmonics were called for in each zone and how their ARIMA error components behaved.

The last modelling framework-The Fourier harmonics and ARIMA errors-provided a comprehensive practical work on a single model pipeline: diagnostics, regress diagnostics, design, decomposition, and forecasting. It reinforced my lean of knowing the physics of the data generating process being modelled and providing reconciling it statistically and with constraint. The project has improved my confidence in actively analysing difficult time series problems of real-world complexity, and with large datasets, weak seasonality, and a complex periodic structure.